Journal of Autoimmunity 32 (2009) 85–93

Contents lists available at ScienceDirect

Journal of Autoimmunity

journal homepage: www.elsevier.com/locate/jautimm

Cellular and humoral immune responses in the early stages of diabetic nephropathy in NOD mice

Xiaoyan Xiao [a,b], Bin Ma [a,c], Baojun Dong [a], Peng Zhao [d], Ningwen Tai [a], Li Chen [b], F. Susan Wong [e,**,1], Li Wen [a,*,1]

[a] Section of Endocrinology, Department of Internal Medicine, Yale School of Medicine, 330 Cedar Street, New Haven, CT 06520, USA
[b] Department of Endocrinology, Qilu Hospital, Shandong University, Jinan, PR China
[c] Department of Microbiology, Langone Medical Center, New York University, NY, USA
[d] Department of Cardiology, Shandong Provincial Hospital, Shandong University, Jinan, PR China
[e] Department of Cellular and Molecular Medicine, University of Bristol, Bristol, United Kingdom

ARTICLE INFO

Article history:
Received 6 November 2008
Received in revised form
11 December 2008
Accepted 17 December 2008

Keywords:
Non-obese diabetic mice
Kidney
Diabetic nephropathy
Immune response

ABSTRACT

This study was designed to examine immunopathology of diabetic nephropathy in non-obese diabetic (NOD) mice and to investigate the involvement of cellular and humoral immunity at various time points after diabetes onset. We found that the glomeruli of diabetic NOD mice were infiltrated with T and B cells, as well as CD11c+ dendritic cells, which had close contact with CD4+ and CD8+ T cells in the infiltrates. We also found that IgG deposits in the glomeruli of diabetic NOD mice were accompanied by the presence of complement C3. Moreover, the serum from diabetic mice contained autoantibodies directed towards components of the glomeruli and these antibodies were not present in non-diabetic NOD mice. The immune changes in the kidney occurred together with increasing kidney weight and urinary albumin excretion along with duration of diabetes. We provide evidence that infiltrating lymphocytes and anti-kidney autoantibodies may be involved in diabetic nephropathy in autoimmune diabetes in the NOD mouse. Understanding the role that the immune system plays in the pathogenesis of diabetic nephropathy could lead to identification of new strategies and/or additional therapeutic targets for prevention and treatment of diabetic nephropathy.

1. Introduction

Diabetic nephropathy is the leading cause of end-stage renal failure in young people and affects about 40% of individuals with long-standing type 1 diabetes [1]. Current therapy, which includes treatment for hyperglycemia, hypertension and dyslipidemia can slow the rate of progression of diabetic nephropathy [2], but eventually end-stage renal failure will still occur in a proportion of patients [3]. Therefore, the effects of currently used treatments must be maximized and identification of new strategies and additional therapeutic targets for treating diabetic nephropathy will be important.

Many factors are involved in the pathogenesis of diabetic nephropathy, which in humans is defined by a progressive rise in albuminuria, together with increasing blood pressure, leading to a fall in glomerular filtration and ultimately end-stage renal failure [3]. Microalbuminuria may occur as early as 5 years after diagnosis of diabetes [3]. Structural abnormalities include glomerular basement membrane thickening, increased number of mesangial cells and mesangial expansion [4]. Metabolic factors, such as the formation of advanced glycation end products and increased flux through the polyol pathways, have been implicated [5]. In addition, growth factors (transforming growth factor TGF-β, insulin-like growth factor IGF-1 and vascular endothelial growth factor VEGF) may also play a role [5,6]. Although the pathogenesis of diabetic nephropathy is not considered to be primarily immune mediated, nevertheless studies examining renal biopsies in patients with type 1 diabetes have noted T cell infiltration of the juxtaglomerular apparatus [7,8]. Macrophages have also been detected in kidney sections from patients with diabetic nephropathy although no distinction was made between patients with type 1 or type 2 diabetes [9].

To facilitate dissection of pathogenesis of diabetic nephropathy, a variety of experimental rat and mouse models have been used, many of which relate to type 2 diabetes. In the present study, we

* Corresponding author. Tel.: +1 203 785 7186; fax: +1 203 737 5558.
** Corresponding author. Tel.: +44 117 331 2079; fax: +44 117 928 7896.
E-mail addresses: susan.wong@bristol.ac.uk (F. Susan Wong), li.wen@yale.edu (L. Wen).
[1] F.S. Wong and L. Wen contributed equally to this study.

0896-8411/$ – see front matter © 2009 Elsevier Ltd. All rights reserved.
doi:10.1016/j.jaut.2008.12.003

focused on the non-obese diabetic (NOD) mouse model that develops spontaneous autoimmune diabetes similar to human type 1 diabetes [10]. Many studies of diabetic nephropathy were performed in chemically-induced diabetic animal models and NOD mice have not been studied much in terms of diabetic nephropathy, perhaps because of the potentially long and variable time to onset of diabetes [11]. However, a few studies have shown that NOD mice could develop renal pathology after the onset of diabetes [12,13]. To test the hypothesis that immune responses are involved in the development of diabetic nephropathy, we investigated cellular and humoral immune parameters in spontaneous diabetic NOD mice.

2. Materials and methods

2.1. Animals

Female NOD/Caj mice were used in this study. All the mice were housed in individually-ventilated filter cages with autoclaved food under specific pathogen-free (SPF) conditions with a 12-h dark/light cycle. The use of the animals and the procedures applied in this study were approved by the Institutional Animal Care and Use Committee of Yale University.

2.2. Determination of diabetes and diabetic nephropathy

NOD mice were observed for diabetes development by weekly screening for glycosuria. Diabetes was confirmed following 2 consecutive readings of blood glucose greater than 13.9 mmol/L (250 mg/dl). Mouse urine was screened for proteinuria by Albustix (Bayer, Elkhart, IN, USA). Diabetic mice were given a sub-therapeutic dose of insulin (Eli Lilly, Indianapolis, IN, USA) after diagnosis in order to maintain the animals in a hyperglycemic state, in the range of 13.9–22.2 mmol/L, but in relatively good general health. Blood glucose and proteinuria were monitored weekly. Twenty-four hour urine collections were obtained using metabolic cages and quantitation of urine albumin was determined using the Protein Assay Kit from Bio-Rad (Hercules, CA, USA) according to the manufacturer's instructions. The urine creatinine was measured by Cayman creatinine assay kit (Ann Arbor, MI, USA).

2.3. Histology

Mice were perfused with ice-cold PBS and then with buffer containing 10% formalin. Tissues were further fixed in 4% buffered paraformaldehyde for 2 days, embedded in paraffin and processed for sectioning. Extracellular matrix deposition in glomeruli was assessed by Periodic Acid-Schiff (PAS) staining.

2.4. Immunofluorescent labeling and confocal microscopy

Perfused kidney was fixed overnight in periodate–lysine–paraformaldehyde (PLP) fixative (2% paraformaldehyde, 0.075 M lysine, 0.037 M sodium phosphate, 0.01 M periodate). The tissue was then embedded in OCT compound from Tissue-Tek (Torrance, CA, USA) and snap frozen. Cryosections (10 μm) were rehydrated with PBS followed by blocking with 2% goat serum (Sigma Immunochemicals, St. Louis, MO, USA). The following primary antibodies were used for staining the kidney sections: phycoerythrin (PE)-conjugated donkey anti-mouse IgG and rat anti-mouse CD31 (eBioscience, San Diego, CA, USA), rabbit anti-mouse laminin (Meridian Life Science, Saco, ME, USA), rat anti-mouse CD4 (Invitrogen, Carlsbad, CA, USA), fluorescein isothiocyanate (FITC)-conjugated rat anti-mouse CD11c, rat anti-mouse CD8 (Invitrogen, Carlsbad, CA, USA), rabbit anti-mouse perforin antibody (Cell Signaling, Beverly, MA), rat anti-C3 antibody (Cedarlane, Burlington, NC, USA). Secondary antibodies (goat anti rat Alexa 488, 546; goat anti-rabbit Alexa 488, goat anti FITC Alexa 488 were obtained from Invitrogen, Carlsbad, CA, USA, and goat anti-rabbit Cy5 at1:300 were obtained from Abcam (Cambridge, MA, USA). Kidney sections were examined and photographed using a META510 confocal microscope (Carl Zeiss, Thornwood, NY, USA). Images were acquired with a 63× water-immersion objective lens. For some micrographs, Tile Scan was performed to obtain high-resolution images from large areas of the organ.

2.5. Electron microscopy

After perfusion the kidneys were excised and immersed in fresh fixatives (2.5% glutaraldehyde in 0.1 M Na cacodylate buffer, pH 7.4) for ∼16 h at 4 °C. For morphological studies, the tissue blocks were post-fixed with 1% osmium tetroxide/0.8% potassium ferricyanide in 0.1 M cacodylate buffer, treated with aqueous 1% uranyl acetate, dehydrated in graded ethanol solutions, and embedded in Polybed epoxy resin (Polysciences, Warrington, PA, USA). Thin sections were cut, collected on 200 mesh copper/rhodium grids, and stained with uranyl acetate and lead citrate and then were observed at 60 kV in a Philips CM10 transmission EM.

For immunogold labeling, osmium post-fixation was omitted, and the tissue blocks were embedded in LR Gold acrylic resin, and polymerized with UV light at −20 °C. The sections were treated with bovine serum albumin (BSA), with or without normal goat serum (the species in which the secondary antibody was raised), in PBS with 0.1% Tween 20 to block non-specific binding, then incubated with rabbit anti-mouse IgG (Jackson ImmunoResearch, West Grove, PA, USA) or goat anti-mouse IgG (KPL, Gaithersburg, MD, USA) overnight at 4 °C. After rinsing with PBS, the sections were incubated with a gold-labeled secondary antibody – 15 nm gold-labeled goat anti-rabbit IgG (Aurion, Wageningen, Netherlands) for 60 min at room temperature. Following rinse with PBS and distilled water, the sections were stained with uranyl acetate and lead citrate and examined in a Philips CM10 transmission electron microscope.

2.6. RNA extraction and real-time quantitative PCR

Total RNA was isolated from mouse kidney tissues using TRIzol (Invitrogen, Carlsbad, CA, USA). Equal amounts of RNA, measured by spectrophotometer and RNA gel, were used for first-strand cDNA synthesis with SuperScript III-RT kit (Invitrogen, Carlsbad, CA, USA) in a 20 μl reaction. 0.5 μl of cDNA product was then subject to the quantitative PCR (qPCR) amplification. The primers were designed using the Primer Bank (http://pga.mgh.harvard.edu/primerbank/) and synthesized by Sigma. Real-time quantitative PCR was performed using an iCycler system (Bio-Rad, Hercules, CA, USA) and SYBR green I was used to detect the PCR products. The integrity of DNA products was verified by both the presence of a single melting temperature peak and a single band on a 1.2% agarose gel. Post-PCR data were analyzed by the iQ™ 5 optical system software (Bio-Rad, Hercules, CA, USA). Relative quantification was determined using $2^{-\Delta\Delta C_t}$ method with data normalized to the mRNA level of housekeeping gene GAPDH.

2.7. Determination of anti-insulin autoantibodies

The serum samples of diabetic NOD mice were tested for the presence of anti-insulin autoantibodies before and after the onset of diabetes and institution of insulin treatment as previously described [14].

2.8. Statistical analysis

The data were presented as means ± SD or means ± SE. Statistical analysis was performed using GraphPad Prism software 4.0 (San Diego,

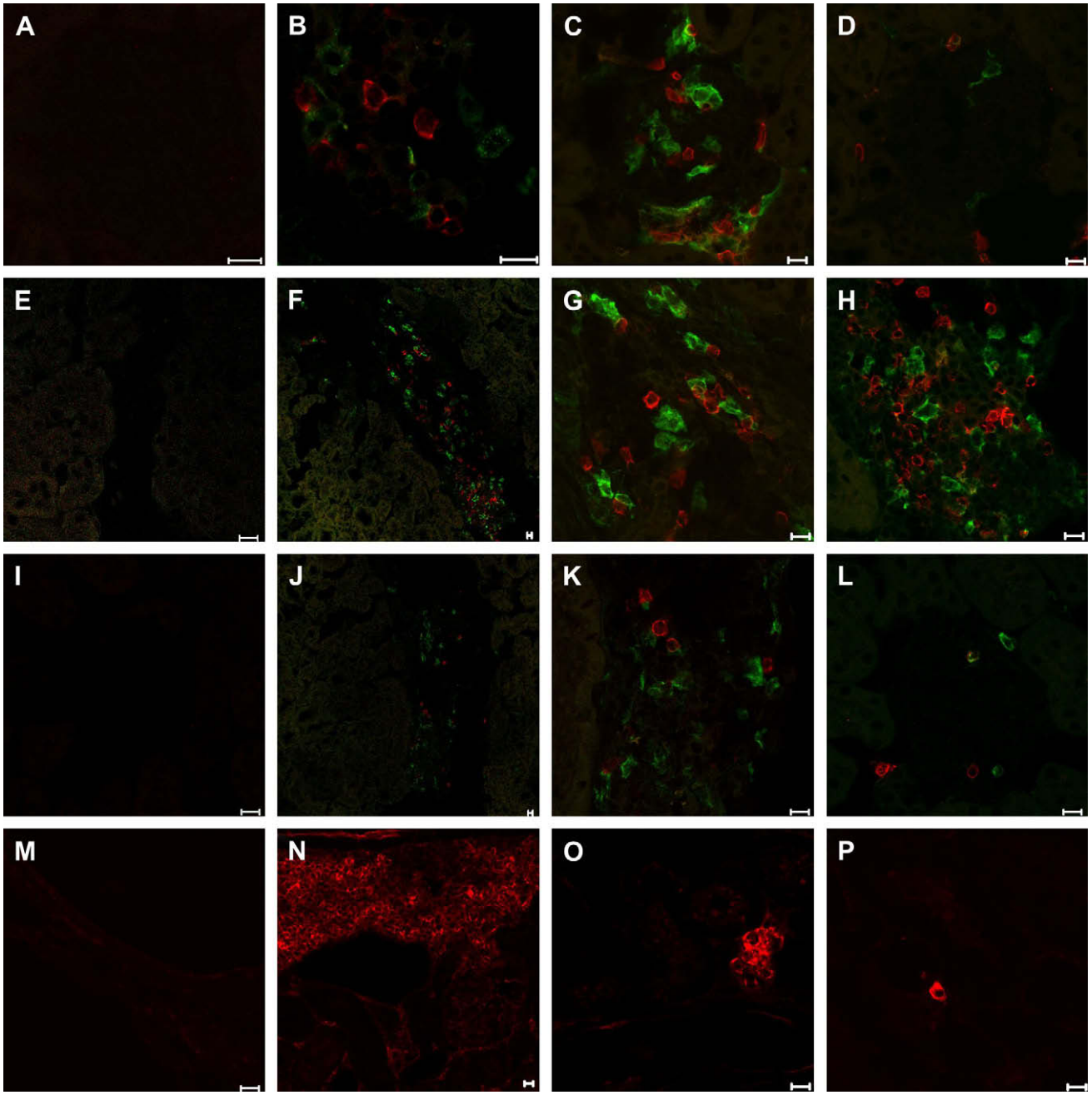

Fig. 1. Immuno-fluorescence staining of immune cells in kidneys from NOD mice at different times after onset of diabetes. Confocal analysis showing CD4 cells (red) and CD11c positive cells (green) in kidney sections in (A) a non-diabetic mouse, (B) a mouse diabetic for one month (C) a mouse diabetic for two months (D) a mouse diabetic for three months (D). Further analysis shows CD4 cells (red) and CD11c positive cells (green) in blood vessels in (E) a non-diabetic mouse, and (F) in a diabetic mouse one month after diabetes onset seen under 63× water-immersion objective lens and tile scanned amplification (G and H respectively). CD8 cells (red) and CD11c positive cells (green) in (I) a non-diabetic mouse, in blood vessels in mouse diabetic for 1 month seen under 63× water-immersion objective lens (J), and tile scanned amplification (K), and in the glomeruli (L); IgG positive B cells in (M) a non-diabetic mouse, near blood vessels in a mouse diabetic for one month (N), in a cluster (O) and scattered single IgG positive cells (P). Scale bar 10 μm. $N = 4–6$ for each group.

CA, USA). $P < 0.05$ was considered significant. *T* test or one way ANOVA was performed wherever appropriate. Post-hoc Bonferroni pairwise comparison was followed to assess significance between two groups.

3. Results

3.1. Cellular immune responses in diabetic kidneys

To investigate whether cellular immune responses are involved in the pathogenesis of diabetic nephropathy, we examined mononuclear cell infiltration in glomeruli with confocal microscopy at monthly intervals after the development of diabetes. All the kidneys were perfused before preparation of tissue sections. We found that CD4+ (Fig. 1B–D, F–H) and CD8+ (Fig. 1J–L) T cells were present in the glomeruli in diabetic mice. Dendritic cells (CD11c+) were also present in the infiltrates, in close contact with both CD4 (Fig. 1B–D, F–H) and CD8 T cells (Fig. 1J–L). In addition, heavy lymphocytic infiltration including IgG+ B cells could also be found close to blood vessels (Fig. 1N). IgG+ B cells were either in clusters or scattered individually (Fig. 1O–P). In sharp contrast, no immune

cell infiltration was seen in glomeruli or other parts of the kidney from non-diabetic control mice (Fig. 1A,E,I,M).

3.2. mRNA expression of perforin and granzyme B and co-localization of perforin with CD8+ T cells

CD8+ T cells use release of perforin and granzyme B for their cytolytic function. We evaluated perforin and granzyme B mRNA expression in the kidney by real-time PCR. Total cellular RNA was isolated from the renal cortex of diabetic and non-diabetic mice. Fig. 2A demonstrated a significant increase of perforin and granzyme B mRNA expression in the renal cortex in diabetic animals compared with non-diabetic animals ($P < 0.01$). This was further confirmed by confocal microscopy showing co-localization of CD8 and perforin staining (Fig. 2B and Supplementary 3D movie), whereas neither CD8+ T cells nor perforin could be found in the kidneys of non-diabetic NOD mice (Fig. 2B).

3.3. Humoral immune responses in diabetic kidneys

As IgG+ B cells were found in the glomeruli of diabetic NOD mice, to identify whether secreted IgGs were also present in the glomeruli, we stained the diabetic kidney sections with fluorescence-conjugated anti-mouse IgG. As shown in Fig. 3A, IgG deposition was found in kidney sections of all stages of diabetes (1–3 months after clinical onset). In sharp contrast, there was no IgG staining if the kidney sections from non-diabetic NOD mice were used (Fig. 3A). The IgG found in the glomeruli may be produced by the infiltrating B cells in situ (Fig. 3A) or deposited from the circulation (see below). It is interesting that the IgG deposition was associated with CD31, which is expressed on endothelial and inflammatory cells, and laminin, the major non-collagenous component of the basal lamina, as shown in Fig. 3B, C. The association of IgG deposition with CD31 and laminin suggests that the IgG deposits are likely to be on endothelial cells and glomerular basement membrane (GBM). To further investigate the IgG deposition, we performed electron microscopy with immunogold staining, in which the secondary antibody was labeled with gold. As shown in Fig. 3D, most of the gold was present over deposits that were located in and around mesangial cells or between mesangial cells and endothelial cells. Gold particles were also present over the GBM (Fig. 3D). In addition, some gold particles were found in the cytoplasm or lysosomes of mesangial-like cells, which suggested that these cells may have endocytosed IgG (Fig. 3D). There was no gold staining in kidneys from non-diabetic mice (Fig. 3D).

3.4. Diabetic NOD mice produce autoantibodies

To further investigate the IgG found in kidneys of diabetic NOD mice, we examined serum samples from diabetic and non-diabetic NOD mice. Using perfused kidney sections from normal non-diabetic mice, we incubated the sections with serum samples taken from mice at different times after the onset of diabetes followed by fluorescence-labeled goat anti-mouse IgG as detecting antibody. It is interesting that IgG staining was only found in the sections when serum samples from diabetic mice were used as primary antibody (Fig. 4A) whereas there was no IgG staining when non-diabetic mouse sera were used (Fig. 4B). As the mice were treated with human insulin after the onset of diabetes, we tested for the presence of anti-insulin autoantibodies to ascertain if anti-insulin antibodies forming immune complexes were responsible for the deposition in the kidneys. However, there was no obvious

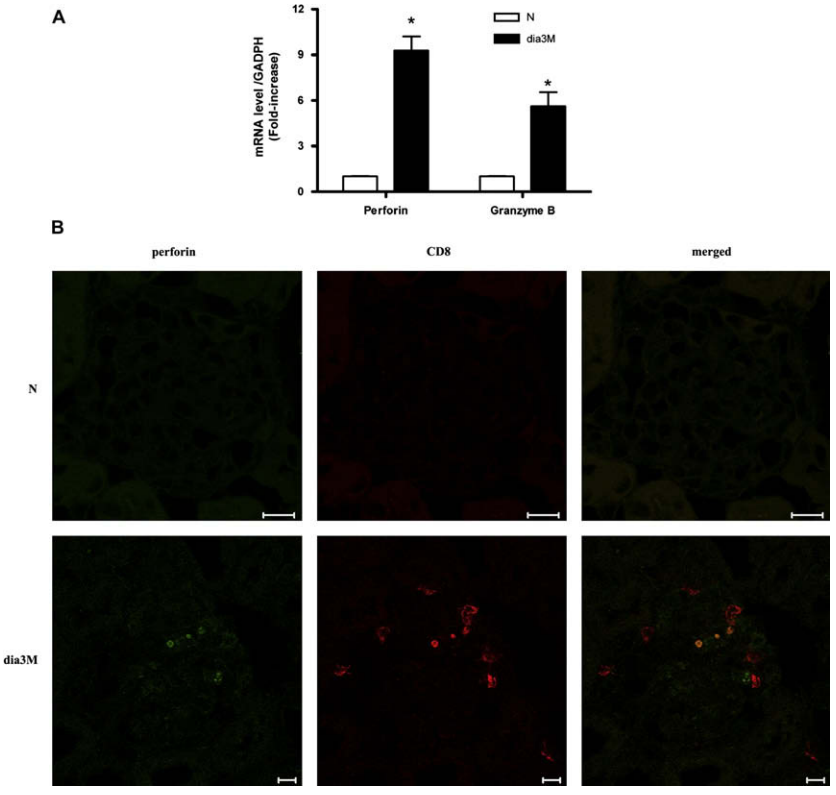

Fig. 2. Presence of perforin and CD8 cells in diabetic kidneys. A: Perforin and granzyme B expression levels in the kidney of non-diabetic control mice compared with kidneys from NOD mice diabetic for 3 months. Gene expression was normalized with GADPH and expressed as fold increase relative to the non-diabetic control mice. N, non-diabetic control; dia 3M, mice diabetic for 3 months, $^{*}P < 0.01$ vs. N. Each column consists of means ± SE, $n = 4$ for each group. B: Perforin staining is colocalized with cells stained for anti-CD8 in non-diabetic and diabetic mice. Double-fluorescence analysis revealed perforin (green) and CD8 (red) in the glomerulus of a mouse diabetic for 3 months, merging of both channels green and red was seen as yellow. Scale bar 10 μm. $N = 4$ for each group.

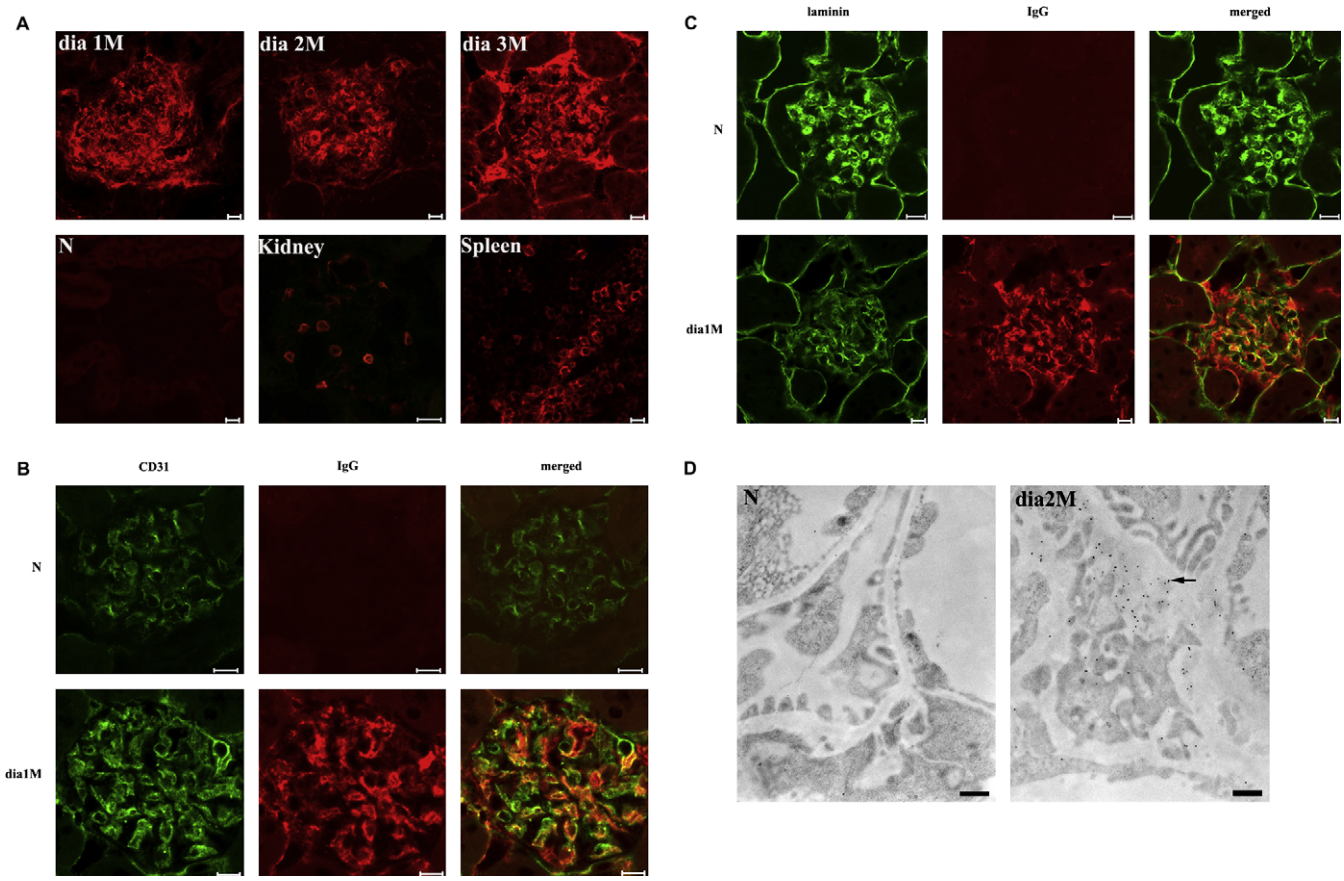

Fig. 3. IgG deposition in kidneys of diabetic NOD mice A: IgG deposits were assessed by anti-mouse IgG and examined using confocal microscopy (with Tile scan) in NOD mice diabetic for one month (dia 1M), two months (dia 2M), three months (dia 3M), a non-diabetic control (N), IgG positive B cells in the glomerulus of a mouse diabetic for 2 months (Kidney) and a positive control for IgG positive splenic B cells (Spleen). B: IgG deposits were associated with CD31 in glomeruli from a non-diabetic mouse (N) and a mouse diabetic for 1 month (dia 1M) as shown by staining with anti-CD31 (green), anti-IgG (red), and a merged view (yellow). C: IgG deposits were associated with laminin in glomeruli from a non-diabetic mouse (N) and a mouse diabetic for 1 month (dia 1M) as shown by staining with anti-laminin (green), anti-IgG (red), and a merged view (yellow). Original magnification ×400, and scale bar 10 μm. $N = 5–9$ for each group. D: Electron micrographs of immunogold staining for IgG in a non-diabetic control mouse (N) and a mouse that had been diabetic for two months (dia 2M). Gold granules (arrow) were densely packed within the subendothelial region and glomerular basement membrane. Scale bar 0.5 μm. $N = 2$ for each group.

correlation between the presence of IgG binding in the kidney sections and the presence of anti-insulin autoantibodies in the serum of these mice (data not shown).

3.5. Complement staining associated with IgG deposition

IgG deposition in the kidney suggests the reaction of antibody with antigen and formation of immune complexes (IC), and IC could activate the complement (C) cascade. We next examined for the presence of complement components. NOD mice express normal levels of C3, although they are deficient in C5 [15]. We therefore tested for the presence of C3 in glomeruli using confocal microscopy. We also stained IgG and laminin in the consecutive kidney sections and the results indicated that C3 staining was associated with IgG deposition and laminin (Fig. 5).

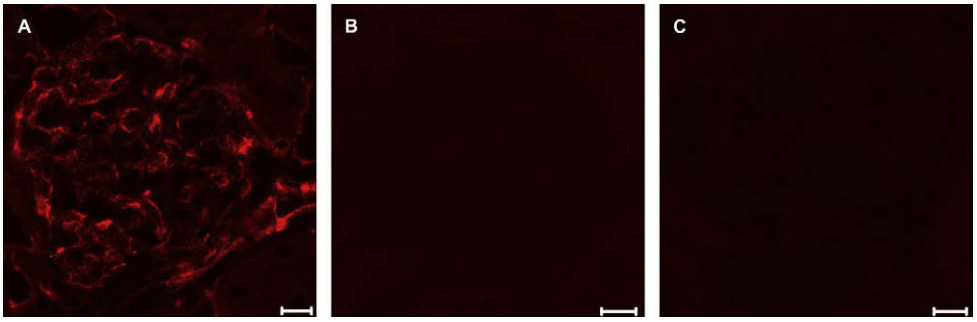

Fig. 4. Autoantibodies are found in sera of diabetic NOD mice. Kidney (perfused) sections from non-diabetic NOD mice were stained with (A) diabetic mouse sera as primary antibody and PE labeled goat anti-mouse IgG as secondary antibody (B) non-diabetic mouse sera as primary antibody and PE labeled goat anti-mouse IgG as secondary antibody (C) secondary PE conjugated goat anti-mouse IgG alone; scale bar 10 μm. $N = 8$ for each group.

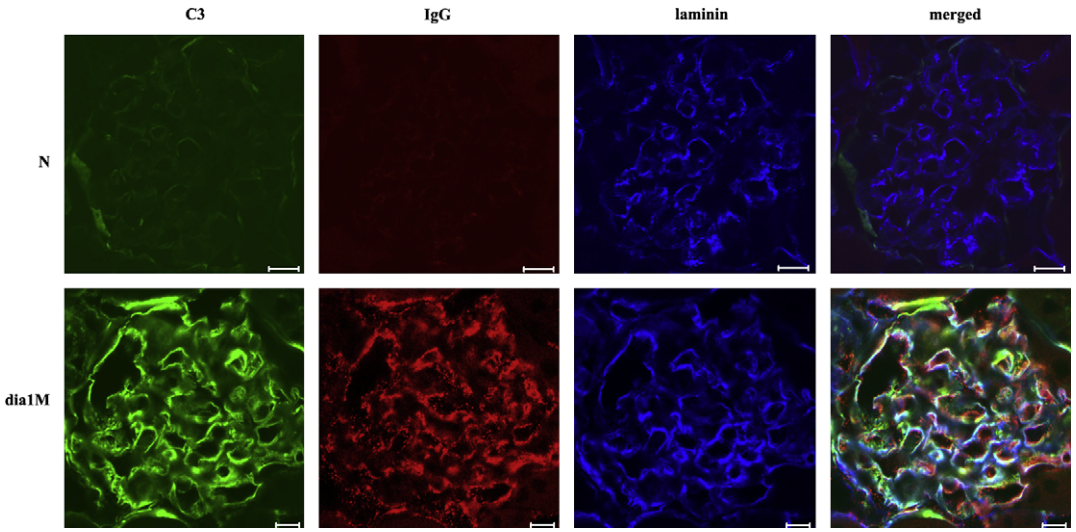

Fig. 5. C3 deposits in the kidney of diabetic NOD mice. C3 deposition was assessed by immunofluorescent staining of perfused kidney sections from non-diabetic mice (N) and diabetic mice for 1 month (dia 1M). Three-color immuno-fluorescence analysis shows C3 deposits (green), IgG (red) and laminin (blue) and with merging of all channels. Scale bar 10 μm. $N = 6$ for each group.

3.6. Kidney hypertrophy and urinary albumin excretion in diabetic NOD mice

To further document renal changes after the onset of diabetes, we found that the normalized kidney weight increased with the duration of diabetes in NOD mice, implying kidney hypertrophy (Fig. 6A). It is interesting that the normalized kidney weight remained unchanged one month post diabetes onset but the weight significantly increased two months after disease onset with a further increase after three months, at which time the experiments were terminated (Fig. 6A). Although kidney hypertrophy did not occur one month after diabetes onset in these mice, urinary albumin excretion rate (UAE) had significantly increased at that time (Fig. 6B). UAE was further elevated at two months and remained at the same level by three months when the experiment was terminated (Fig. 6B), while the normalized kidney weight of these mice continued to increase significantly ($P < 0.01$, Fig. 6A). The mean blood glucose over this time remained unchanged with sub-therapeutic doses of insulin during the three-month experimental period (Fig. 6C, $P > 0.05$), although the glucose level was significantly higher, as expected, than in non-diabetic control NOD mice (Fig. 6C, $P < 0.001$).

3.7. Glomerular hypertrophy and mesangial matrix expansion

As one of the hallmarks of diabetic nephropathy is mesangial matrix expansion, we investigated the progression of mesangial matrix expansion in diabetic NOD mice by analyzing the kidney sections obtained at different time points after diabetes onset. As shown in Fig. 7A, glomerular hypertrophy and accelerated mesangial matrix expansion progressed with duration of the disease, which was characterized by an increased area(s) positive for PAS staining compared with non-diabetic controls. To further investigate the structural changes of the glomeruli, especially the GBM, we performed transmission electron microscopy. The GBM was thicker in diabetic mice compared with non-diabetic controls and the alterations in thickness were irregular and regional (Fig. 7B). We also found extracellular matrix accumulation in diabetic kidneys under electron microscopy (Fig. 7B).

4. Discussion

Our study has shown that, firstly, in the early stages of diabetes in the NOD mouse, both T and B cells infiltrate the glomeruli. Secondly, we have demonstrated that serum components from

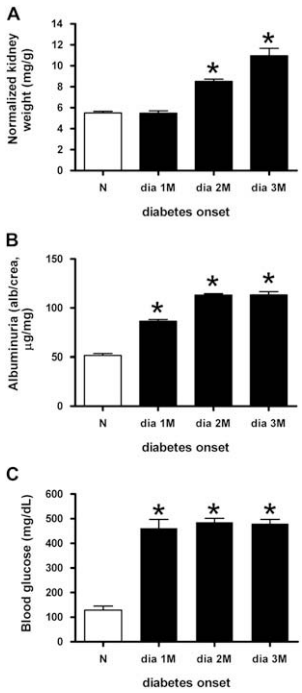

Fig. 6. Natural history of changes in kidney weight and albuminuria with time after onset of diabetes. A: Increase in kidney weight to body weight ratio in NOD mice is shown. $^*P < 0.01$ vs. non-diabetic mice (N), $n = 8$ for each group. Each column represents the mean ± SD. B: Urinary albumin excretion, related to creatinine over 24 h is shown at months 1, 2, 3 after onset of diabetes. $^*P < 0.01$ vs. N, $n = 5$–8 for each group. Each column represents the mean ± SD. C: Average blood glucose in diabetic NOD mice compared to non-diabetic NOD mice. $^*P < 0.001$ vs. N, $n = 8$ for each group. Each column represents the mean ± SD. N, non-diabetic control; dia 1M, one month after diabetes onset; dia 2M, two months after diabetes onset; dia 3M, three months after diabetes onset.

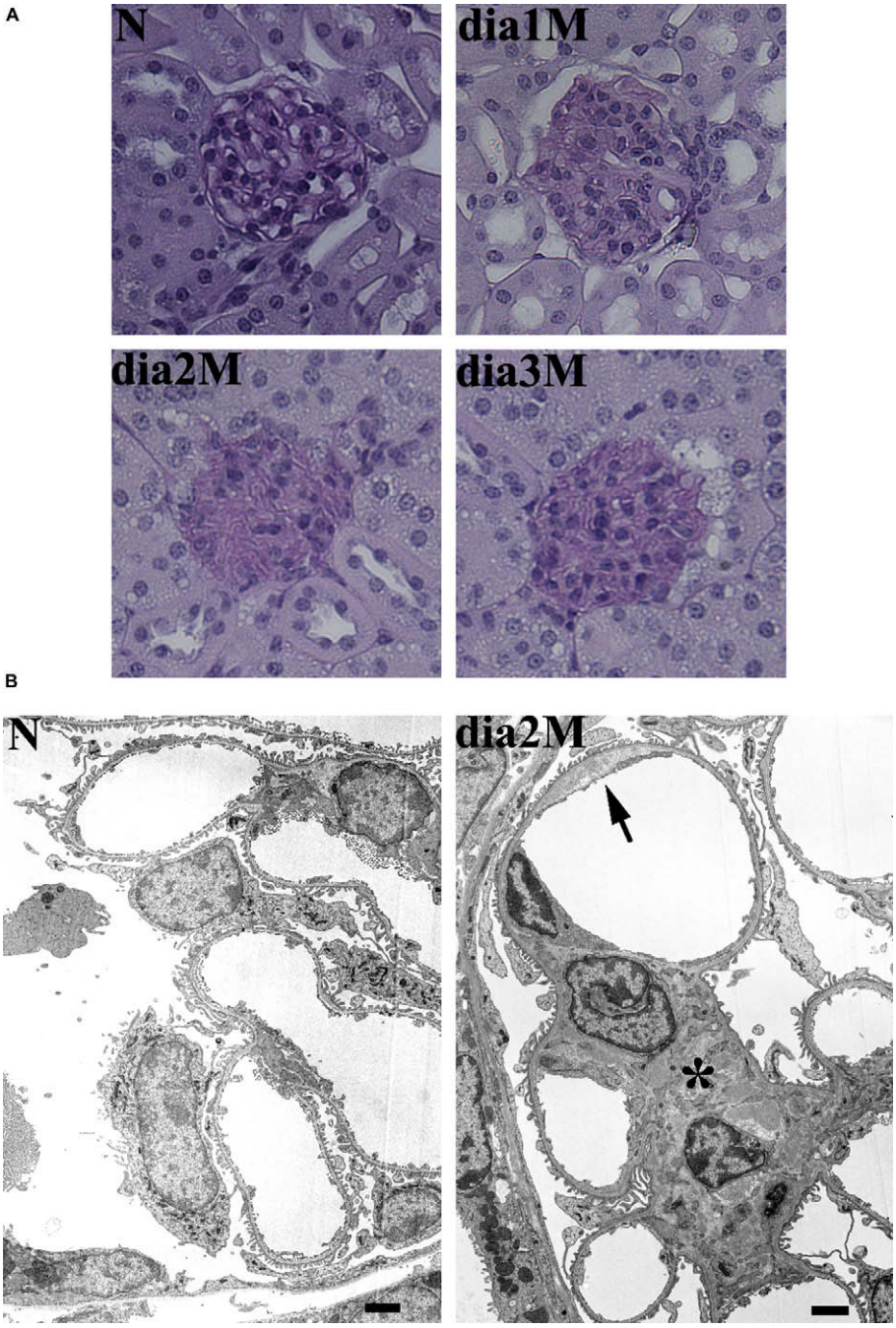

Fig. 7. A: Periodic Acid-Schiff (PAS) staining of kidney sections from non-diabetic and diabetic NOD mice. Representative light microscopic appearance of glomeruli (PAS staining; original magnification ×200) for N, non-diabetic control; dia 1M, one month after diabetes onset; dia 2M, two months after diabetes onset; dia 3M, three months after diabetes onset. Matrix thickening was seen in the glomeruli. $N = 6$ for each group. B: Electron micrographs of glomeruli in a non-diabetic control (N), and a diabetic mouse, 2 months after diabetes onset (dia 2M). Matrix accumulation (*) and irregular thickening of the glomerular basement membrane (arrow) were observed in the glomeruli. Scale bar 2 μm. $N = 2$ for each group.

diabetic NOD mice, but not non-diabetic NOD mice, bind to normal kidney sections, indicating the presence of autoantibodies to the kidney. These autoantibodies only develop after the mice become diabetic and appear to be directed towards renal endothelial cells and the glomerular basement membrane. Thirdly, we have shown the presence of complement C3 deposits in the kidney. Fourthly, in documenting the natural history of renal changes in the NOD mouse after the onset of autoimmune diabetes, we have shown that UAE started to increase after 1 month of diabetes, with further increases as the duration of diabetes increased. Furthermore, the kidney weight increased, together with evidence of mesangial expansion, and this is consistent with renal hypertrophy occurring after at least 1 month of hyperglycemia.

There has, thus far, been limited knowledge about immune cell recruitment into renal tissues in diabetic nephropathy, although recent studies have suggested a role for immune cells in diabetic nephropathy [16]. In patients with type 1 diabetes, the presence of nephropathy has been associated with increased activated peripheral blood T cells [17] and more recently, infiltration of T cells into the kidney [8]. In addition, other indicators

of inflammation in serum such as mannan-binding lectin are also associated with diabetic nephropathy [18–20]. Furthermore, T cells that have receptors for advanced glycation end products (AGEs) have been shown to produce interferon-γ upon interaction with AGEs [21] and if attracted into the kidney they could contribute to local inflammation and tissue damage. We found that both CD4 and CD8 T cell infiltration together with CD11c cells in glomeruli in diabetic NOD animals. Not only do NOD mice develop diabetes, but they also have immune cell infiltration in the salivary glands, thyroid, adrenal glands and reproductive organs [22]. Unlike the spontaneous lymphocytic infiltration into these organs, we have shown that lymphocyte infiltration and tissue damage in kidney only occurs after development of diabetes and this may indicate that there is an immune component associated with the development of proteinuria in diabetic nephropathy to which individuals are genetically susceptible but that requires an important trigger in the form of hyperglycemic damage or an environmental insult [23].

In addition to the lymphocytic infiltrate, we have also observed antibody deposits within the kidney, particularly in the glomeruli and related to CD31 and laminin. Immunogold electron microscopy indicated that the IgG deposits were subendothelial and mesangial deposits. Such deposits tend to occur in tandem, leading to active inflammation when deposits are extensive. Immunogold electron microscopy also demonstrated the deposition of IgA in the kidney (data not shown). They occur later than IgG, and are possibly associated with a later stage of immune response as class switching to IgA normally takes place after IgG.

It is interesting that serum from diabetic mice contained antibodies that reacted to kidney components whereas this was not seen in the sera from non-diabetic mice. Preliminary western blot analysis indicated that proteins of two different molecular weights around 30 and 60 kD were immunoprecipitated (data not shown) but at this time, it is not known what the proteins are and this will be a focus of future study.

The association of circulating immune complexes with diabetic complications has been studied in the past with suggestions that increased levels of immune complexes are found in patients with diabetic microangiopathic complications, including oxidized LDL-anti-oxidized LDL immune complexes [24–26]. It is not clear whether immune complexes with insulin are contributory to microangiopathic complications [27]. In the present study, we gave a small dose of human insulin to maintain diabetic animals but we found no obvious correlation between the presence of IgG binding in the kidney sections and the presence of anti-insulin autoantibodies in circulation, indicating that the antibodies in the IgG found in the kidney were not due to immune complexes associated with insulin autoantibody in this model.

In this study, we demonstrated glomerular IgG and C3 in diabetic NOD kidneys as diabetes developed. Notably, age-matched NOD mice that did not develop diabetes showed no deposition of IgG or C3 in the glomeruli compared to diabetic animals, implying that IgG and C3 deposition in glomeruli is associated with diabetes rather than the genetic make-up of these animals. Activation of the complement system has also been reported to play a pathogenic role in human diabetic nephropathy [19,20,28]. NOD mice have no complement lytic activity as they lack C5 due to a two-base pair deletion in the coding region of *Hc* and therefore, the complement pathway cannot be activated [15]. However, they have normal levels of C3, which could be involved in the activation of the autoreactive B cell populations via the C3d component [29].

In humans, the increase in UAE is predominantly related to abnormalities in the glomerulus [3]. In our study we demonstrated increased UAE, together with histological changes of irregular basement membrane thickening and mesangial expansion. However, this may also be due to metabolic changes in addition to the immune abnormalities.

In conclusion, the present studies provide strong evidence for the involvement of cellular and humoral immune responses in the early stages of diabetic nephropathy in NOD mice.

Although further investigation should focus on the identification of antigens which initiate the immune response, our results from this study substantially extend recent reports indicating that immune responses play an important role in diabetic nephropathy. Further elucidation of mechanisms of immune-mediated damage will hopefully lead to new therapeutic strategies and/or additional therapeutic targets for prevention and treatment of diabetic nephropathy.

Acknowledgements

Xiaoyan Xiao is a scholarship recipient from the China Scholarship Council (2007-102113). This study was supported by an innovative partnership grant to Li Wen and F. Susan Wong from the JDRF (19-2006-1075). We are grateful to Arthur Hand (University of Connecticut) for the electron microscopy work, Octavian Hengariu for measurement of insulin autoantibodies, Jan Czyzyk for help with independent evaluation of nephropathy and Bin Lu for help with animal care.

Appendix. Supplementary data

Supplementary data associated with this article can be found, in the online version, at 10.1016/j.jaut.2008.12.003.

References

[1] Gross JL, de Azevedo MJ, Silveiro SP, Canani LH, Caramori ML, Zelmanovitz T. Diabetic nephropathy: diagnosis, prevention, and treatment. Diabetes Care 2005;28:164–76.
[2] Perkins BA, Ficociello LH, Silva KH, Finkelstein DM, Warram JH, Krolewski AS. Regression of microalbuminuria in type 1 diabetes. N Engl J Med 2003;348:2285–93.
[3] Marshall SM. Recent advances in diabetic nephropathy. Postgrad Med J 2004;80:624–33.
[4] Osterby R, Parving HH, Hommel E, Jorgensen HE, Lokkegaard H. Glomerular structure and function in diabetic nephropathy. Early to advanced stages. Diabetes 1990;39:1057–63.
[5] Schrijvers BF, De Vriese AS, Flyvbjerg A. From hyperglycemia to diabetic kidney disease: the role of metabolic, hemodynamic, intracellular factors and growth factors/cytokines. Endocr Rev 2004;25:971–1010.
[6] Cooper ME. Interaction of metabolic and haemodynamic factors in mediating experimental diabetic nephropathy. Diabetologia 2001;44:1957–72.
[7] Paulsen EP, Burke BA, Vernier RL, Mallare MJ, Innes Jr DJ, Sturgill BC. Juxtaglomerular body abnormalities in youth-onset diabetic subjects. Kidney Int 1994;45:1132–9.
[8] Moriya R, Manivel JC, Mauer M. Juxtaglomerular apparatus T-cell infiltration affects glomerular structure in type 1 diabetic patients. Diabetologia 2004;47:82–8.
[9] Lewis A, Steadman R, Manley P, Craig K, de la Motte C, Hascall V, et al. Diabetic nephropathy, inflammation, hyaluronan and interstitial fibrosis. Histol Histopathol 2008;23:731–9.
[10] Giarratana N, Penna G, Adorini L. Animal models of spontaneous autoimmune disease: type 1 diabetes in the nonobese diabetic mouse. Methods Mol Biol 2007;380:285–311.
[11] Breyer MD, Bottinger E, Brosius 3rd FC, Coffman TM, Harris RC, Heilig CW, et al. Mouse models of diabetic nephropathy. J Am Soc Nephrol 2005;16:27–45.
[12] Maeda M, Yabuki A, Suzuki S, Matsumoto M, Taniguchi K, Nishinakagawa H. Renal lesions in spontaneous insulin-dependent diabetes mellitus in the nonobese diabetic mouse: acute phase of diabetes. Vet Pathol 2003;40:187–95.
[13] Jeansson M, Granqvist AB, Nystrom JS, Haraldsson B. Functional and molecular alterations of the glomerular barrier in long-term diabetes in mice. Diabetologia 2006;49:2200–9.
[14] Hu CY, Rodriguez-Pinto D, Du W, Ahuja A, Henegariu O, Wong FS, et al. Treatment with CD20-specific antibody prevents and reverses autoimmune diabetes in mice. J Clin Invest 2007;117:3857–67.
[15] Baxter AG, Cooke A. Complement lytic activity has no role in the pathogenesis of autoimmune diabetes in NOD mice. Diabetes 1993;42:1574–8.

[16] Ichinose K, Kawasaki E, Eguchi K. Recent advancement of understanding pathogenesis of type 1 diabetes and potential relevance to diabetic nephropathy. Am J Nephrol 2007;27:554–64.
[17] Bending JJ, Lobo-Yeo A, Vergani D, Viberti GC. Proteinuria and activated T-lymphocytes in diabetic nephropathy. Diabetes 1988;37:507–11.
[18] Saraheimo M, Teppo AM, Forsblom C, Fagerudd J, Groop PH. Diabetic nephropathy is associated with low-grade inflammation in Type 1 diabetic patients. Diabetologia 2003;46:1402–7.
[19] Hovind P, Hansen TK, Tarnow L, Thiel S, Steffensen R, Flyvbjerg A, et al. Mannose-binding lectin as a predictor of microalbuminuria in type 1 diabetes: an inception cohort study. Diabetes 2005;54:1523–7.
[20] Saraheimo M, Forsblom C, Hansen TK, Teppo AM, Fagerudd J, Pettersson-Fernholm K, et al. Increased levels of mannan-binding lectin in type 1 diabetic patients with incipient and overt nephropathy. Diabetologia 2005;48:198–202.
[21] Imani F, Horii Y, Suthanthiran M, Skolnik EY, Makita Z, Sharma V, et al. Advanced glycosylation endproduct-specific receptors on human and rat T-lymphocytes mediate synthesis of interferon gamma: role in tissue remodeling. J Exp Med 1993;178:2165–72.
[22] Silveira PA, Baxter AG. The NOD mouse as a model of SLE. Autoimmunity 2001;34:53–64.
[23] Baxter AG, Horsfall AC, Healey D, Ozegbe P, Day S, Williams DG, et al. Mycobacteria precipitate an SLE-like syndrome in diabetes-prone NOD mice. Immunology 1994;83:227–31.
[24] Nicoloff G, Blazhev A, Petrova C, Christova P. Circulating immune complexes among diabetic children. Clin Dev Immunol 2004;11:61–6.
[25] Atchley DH, Lopes-Virella MF, Zheng D, Kenny D, Virella G. Oxidized LDL-anti-oxidized LDL immune complexes and diabetic nephropathy. Diabetologia 2002;45:1562–71.
[26] Virella G, Carter RE, Saad A, Crosswell EG, Game BA, Lopes-Virella MF. Distribution of IgM and IgG antibodies to oxidized LDL in immune complexes isolated from patients with type 1 diabetes and its relationship with nephropathy. Clin Immunol 2008;127:394–400.
[27] Fineberg SE, Kawabata TT, Finco-Kent D, Fountaine RJ, Finch GL, Krasner AS. Immunological responses to exogenous insulin. Endocr Rev 2007;28:625–52.
[28] Ostergaard J, Hansen TK, Thiel S, Flyvbjerg A. Complement activation and diabetic vascular complications. Clin Chim Acta 2005;361:10–9.
[29] Nguyen CQ, Kim H, Cornelius JG, Peck AB. Development of Sjogren's syndrome in nonobese diabetic-derived autoimmune-prone C57BL/6. NOD-Aec1Aec2 mice is dependent on complement component-3. J Immunol 2007;179:2318–29.